

# Simultaneous measurement of the HT and DT fusion burn histories in inertial fusion implosions

A. B. Zylstra, H. W. Herrmann, Y. H. Kim, A. M. McEvoy, M. J. Schmitt, G. Hale, C. Forrest, V. Yu. Glebov, and C. Stoeckl

Citation: *Review of Scientific Instruments* **88**, 053504 (2017); doi: 10.1063/1.4983923

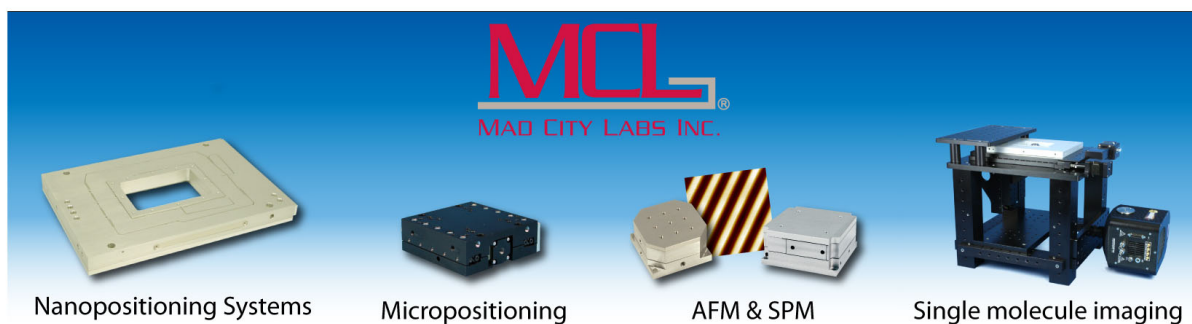
View online: <http://dx.doi.org/10.1063/1.4983923>

View Table of Contents: <http://aip.scitation.org/toc/rsi/88/5>

Published by the *American Institute of Physics*

---

---



# Simultaneous measurement of the HT and DT fusion burn histories in inertial fusion implosions

A. B. Zylstra,<sup>1,a)</sup> H. W. Herrmann,<sup>1</sup> Y. H. Kim,<sup>1</sup> A. M. McEvoy,<sup>1,b)</sup> M. J. Schmitt,<sup>1</sup> G. Hale,<sup>1</sup> C. Forrest,<sup>2</sup> V. Yu. Glebov,<sup>2</sup> and C. Stoeckl<sup>2</sup>

<sup>1</sup>Los Alamos National Laboratory, Los Alamos, New Mexico 87545, USA

<sup>2</sup>Laboratory for Laser Energetics, University of Rochester, Rochester, New York 14623, USA

(Received 27 January 2017; accepted 8 May 2017; published online 23 May 2017)

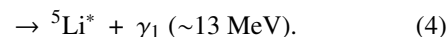
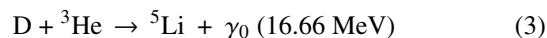
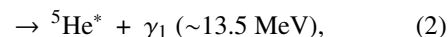
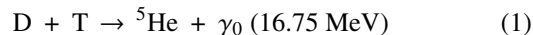
Measuring the thermonuclear burn history is an important way to diagnose inertial fusion implosions. Using the gas Cherenkov detectors at the OMEGA laser facility, we measure the HT fusion burn in a H<sub>2</sub>+T<sub>2</sub> gas-fueled implosion for the first time. Using multiple detectors with varied Cherenkov thresholds, we demonstrate a technique for simultaneously measuring both the HT and DT burn histories from an implosion where the total reaction yields are comparable. This new technique will be used to study material mixing and kinetic phenomena in implosions. *Published by AIP Publishing.* [<http://dx.doi.org/10.1063/1.4983923>]

## I. INTRODUCTION

Inertial confinement fusion (ICF) seeks to create a burning thermonuclear plasma, where the fuel is compressed and heated by spherical implosion.<sup>1</sup> While self-heating has been demonstrated,<sup>2</sup> fusion “ignition” has not been achieved due to a number of degradation mechanisms that limit the implosion performance.<sup>3,4</sup> Experiments towards fusion ignition are ongoing using the National Ignition Facility (NIF)<sup>5,6</sup> and OMEGA<sup>7</sup> laser facilities. One key degradation mechanism in high-convergence implosions is the “mix” of an ablator material into the fuel,<sup>8</sup> caused by hydrodynamic instabilities and diffusion, which can cool the fuel via enhanced bremsstrahlung radiation losses and increased heat capacity of the mixed fuel. This is thought to be one of the dominant degradation mechanisms during the initial high-convergence campaign;<sup>9</sup> understanding and mitigating the mix will be required for ignition. Mix experiments can either directly measure the amount of material introduced into the fuel, or benchmark mix models such as turbulent self-similar growth<sup>10</sup> are often used as an approximation in calculations that cannot fully resolve the hydrodynamics.

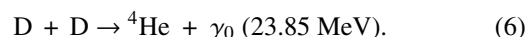
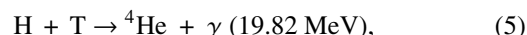
A common experimental platform to diagnose the mix is the separated reactant technique, i.e., where one reactant is in the initial gas fill while the other is within the shell; thus, any yield results from the mixing of the two regions. Usually this mix yield is compared to the yield from a reaction originating only in the gas, representing the clean burn. This technique has been used on the NOVA laser<sup>11</sup> and extensively for the OMEGA<sup>12–15</sup> and NIF.<sup>16–19</sup> A limitation of this technique is that yield measurements are typically integrated over both the spatial and temporal evolutions of the implosion plasma conditions. One study used the measurements of the D<sup>3</sup>He fusion protons to infer the timing of the hydrodynamic mix,<sup>13</sup> but this technique is limited to low areal density implosions that the protons can escape.

In thermonuclear plasmas, the most prevalent<sup>20</sup>  $\gamma$ -ray-producing fusion reactions are



The DT and D<sup>3</sup>He fusion reactions have sufficiently high cross sections and  $\gamma$  branching ratios ( $\sim 0.4 \times 10^{-4}$  for DT<sup>20,21</sup> and  $\sim 1.2 \times 10^{-4}$  for D<sup>3</sup>He<sup>22</sup>) that a large number of  $\gamma$  rays can be produced by implosions. Reactions proceeding directly to the ground states of <sup>5</sup>He and <sup>5</sup>Li produce the highest-energy  $\gamma$  rays from these reactions, at 16.75 and 16.66 MeV, respectively.

Additional reactions that would be useful for implosion diagnostic uses are



Since these reactions produce higher-energy  $\gamma$ 's, they can be discriminated from reactions (1)–(4) by using a high-threshold detector. The DD- $\gamma$  reaction [Eq. (6)] has a very low branching ratio<sup>23</sup> ( $\sim 10^{-7}$ ), but the HT- $\gamma$  reaction has a high enough cross section,<sup>24</sup> and 100%  $\gamma$ -ray branching ratio, that it can be measured. The reactivity and reactivity ratio for HT fusion are shown in Fig. 1, compared to DT and D<sup>3</sup>He. In the temperature range of interest, the HT reactivity is several percent of the DT reactivity.

Since the first excitation energy<sup>25</sup> of <sup>4</sup>He at 20.21 MeV is higher than the  $Q$  value for the HT fusion (19.82 MeV), all reactions proceed to the ground state, resulting in a monoenergetic  $\gamma$ -ray line at a higher energy than that of the DT and D<sup>3</sup>He reactions.

Many separated reactant experiments use hydrogenic reactions, typically the DT and TT fusion reactions, which are measured using neutron diagnostics. Since tritiated shell targets are prohibitively difficult to manufacture, these experiments use deuterated shells with the tritium fuel. While

<sup>a)</sup>Electronic mail: zylstra@lanl.gov

<sup>b)</sup>Present address: Tibbar Plasma Technologies, Los Alamos, New Mexico 87544, USA.

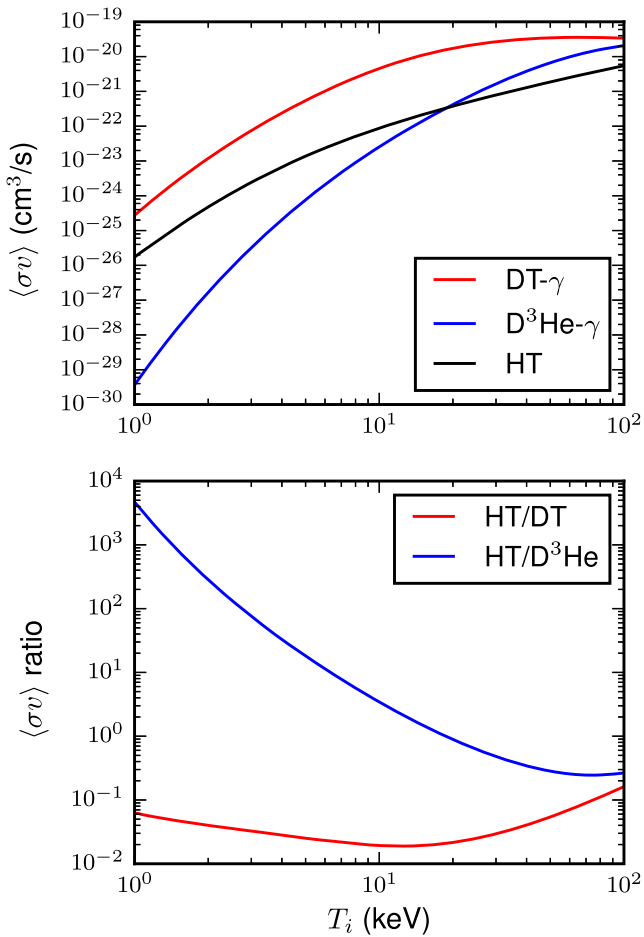


FIG. 1. Top: reactivity for common  $\gamma$ -ray fusion reactions DT and  $D^3\text{He}$  compared to HT. Bottom: the reactivity ratio of HT to DT and  $D^3\text{He}$ .

neutron yield measurements are routine, measuring the relative difference in time between the mix and core burn would be valuable but exceedingly difficult with neutrons, primarily due to the uncertainty in the neutron birth energy.

In this work, we present a new technique for the simultaneous co-timed measurements of the two nuclear burn histories from the  $\gamma$ -ray producing reactions DT and HT, which has been demonstrated at OMEGA. Two Cherenkov detectors with different threshold settings are used to discriminate between the reactions. This can be done relative to a reference shot, as in the work of Rygg *et al.* (Ref. 13), or both burn histories can be measured on a single implosion. Because this measurement uses  $\gamma$  rays, it can also be applied to higher areal density implosions, e.g., ignition-scale experiments on the NIF. Since the mix experiments typically introduce the shell material at a few percent concentration in the burning plasma, in implosions with a HT gas and a deuterated shell, the HT and DT signal levels will be comparable. This new technique adds a measurement of the timing of the mix signal relative to the core burn, which could not be done in the experiments discussed in Refs. 15–19.

This paper is organized as follows: Sec. II discusses the use of thresholded Cherenkov detectors for this measurement, Sec. III demonstrates the first measurement of HT- $\gamma$ 's from an implosion, Sec. IV discusses the analysis of mixed HT- $\gamma$  and DT- $\gamma$  signals, and Sec. V summarizes the work.

## II. CHERENKOV DETECTORS

A description of the Cherenkov detector techniques applicable to this work is given in this section. Several instruments have been developed for the laser-fusion facilities (OMEGA and NIF) based upon the Cherenkov technique.<sup>26–29</sup> In this work, we use the Gas Cherenkov Detectors (GCDs) 1 (Ref. 26) and 3 (Ref. 29). In the GCD incident,  $\gamma$  rays Compton scatter electrons into a gas-filled cell where they exceed the local speed of light ( $c/n$ ), producing Cherenkov radiation that is detected by a photomultiplier tube (PMT). The total PMT integrated signal ( $V \times s$ ) is

$$V \times s = Y_\gamma \times \Omega \times (\chi \times R_{p/\gamma}) \times [\text{QE} \times G \times e \times R_t]. \quad (7)$$

In Eq. (7),  $Y_\gamma$  is the total  $\gamma$ -ray yield and  $\Omega$  is the detector solid angle ( $1.10 \times 10^{-2}$  for the GCDs). The Cherenkov production ( $R_{p/\gamma}$ ) and light collection efficiency ( $\chi$ ) are determined by the detector geometry and gas fill. The electrical response of the system, in square brackets, is the PMT quantum efficiency (QE), its gain ( $G$ ), the fundamental charge ( $e$ ), and the termination resistance ( $R_t = 50 \Omega$ ).

The Cherenkov light production depends upon the incident  $\gamma$ -ray energy and the gas index of refraction, determined by the fill gas type and its density. Response functions are calculated using GEANT4<sup>28</sup> and are shown in Fig. 2. The Cherenkov response increases near the  $\gamma$ -ray energy threshold and continues to increase at a higher energy. Several response curves are shown for  $\text{CO}_2$  gas at 100 psi (absolute) (red curve) and 24–30 psi (absolute) (magenta curves) compared to the DT and HT  $\gamma$ 's. In this work, all pressures are quoted in absolute numbers. Since the DT  $\gamma$  spectrum is dominated by the  $\gamma_0$  and  $\gamma_1$  lines at 16.75 and 13.5 MeV, respectively, reducing the gas density and thereby increasing the Cherenkov threshold will increase the relative sensitivity of the instrument to the higher-energy HT- $\gamma$ 's, albeit at the cost of absolute signal level. For example, at 100 psi (absolute), the response (Cherenkov photons per incident  $\gamma$ ) is  $6.35 \times 10^{-2}$  for DT and  $1.52 \times 10^{-1}$  for HT; at 30 psi (absolute), the response is  $4.72 \times 10^{-3}$  for DT and  $2.73 \times 10^{-2}$  for HT.

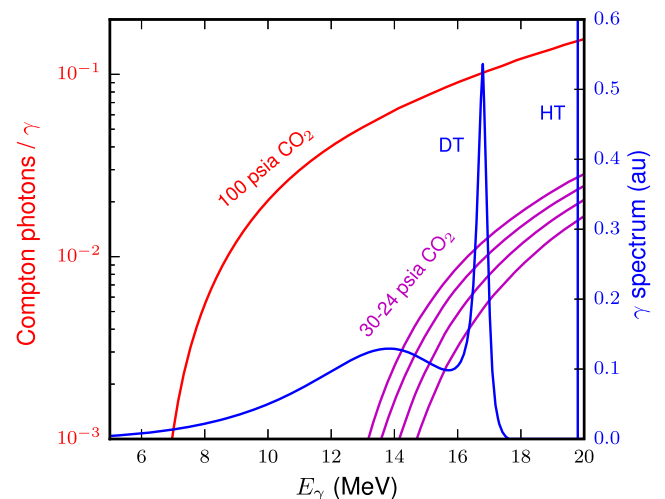


FIG. 2. Cherenkov response (photons per incident  $\gamma$ ) for  $\text{CO}_2$  gas at 100 psi (absolute) (red curve) and 24–30 psi (absolute) (magenta curves). The  $\gamma$ -ray spectrum of DT and HT is shown.

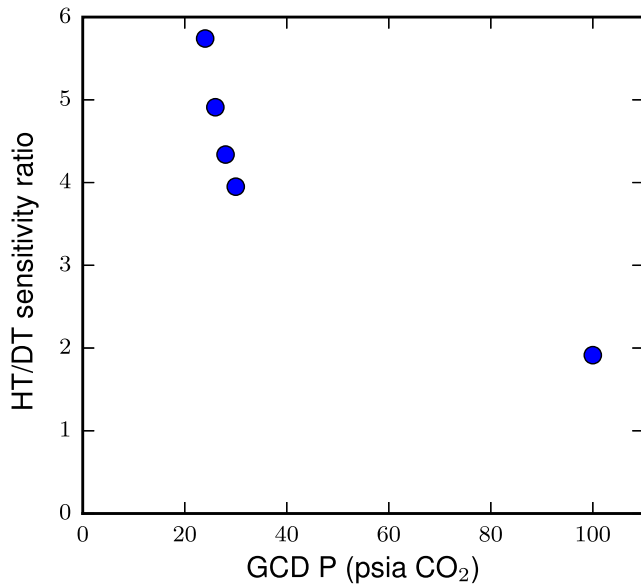


FIG. 3. Ratio of the signal produced per incident  $\gamma$  for the HT to DT reaction versus  $\text{CO}_2$  gas filled pressure.

This is illustrated by calculating the signal ratio for the various response curves from Fig. 2, which is shown in Fig. 3. With 100 psi (absolute) of  $\text{CO}_2$ , the instrument is  $\sim 2\times$  as sensitive to the higher-energy HT  $\gamma$ 's as it is to the DT  $\gamma$ 's (spectrum weighted). If the pressure is reduced to between 30 and 24 psi, then the relative sensitivity increases to 4–6 $\times$ . Thus, if two detectors are used on a shot containing mixed HT and DT signals, one with 30 psi (absolute) fill and the other with 100 psi, the 30 psi (absolute) detector will be more sensitive to the HT reaction, by  $\sim 2\times$ . This use of differentially thresholded Cherenkov detectors forms the basis of the analysis technique discussed in Sec. IV B.

### III. HT- $\gamma$ DEMONSTRATION

HT-produced  $\gamma$  rays generated by inertial fusion implosions were detected for the first time to demonstrate this capability. Implosions were conducted at the OMEGA laser facility<sup>7</sup> using shells filled with equal partial pressures of  $\text{H}_2$  and  $\text{T}_2$ . The  $\text{T}_2$  supply was contaminated with  $\sim 0.1\%$   $\text{D}_2$ , producing a small number of DT fusion reactions. The data from two shots (79 232 and 79 234) are shown in Fig. 4.

The Cherenkov signal is peak-aligned so that the peak nuclear production occurs at  $t = 0$ . The subsequent peaks, starting several hundred ps later, are due to the “ringing” of the PMT, which is caused by an impedance mismatch. A small peak approximately 0.75 ns before the main signal is caused by the direct interaction of  $\gamma$  rays with the PMT<sup>29</sup> (“precursor”). The total integrated signal ( $V \times s$ ), typically determined by a fit, is related to the total  $\gamma$ -ray yield [see Eq. (7)]. Each shot is shown normalized to the DT neutron yield, which is measured using time-of-flight detectors.<sup>30</sup> The expected Cherenkov signal per DT-n is well characterized in previous experiments<sup>20</sup> and is shown as the blue dashed and red dotted curves. Because of the high-purity fill, and thus low DT yield, the HT- $\gamma$  signal is  $\sim 30\times$  the DT- $\gamma$  signal. This represents clear evidence for the detection of HT- $\gamma$ 's. The

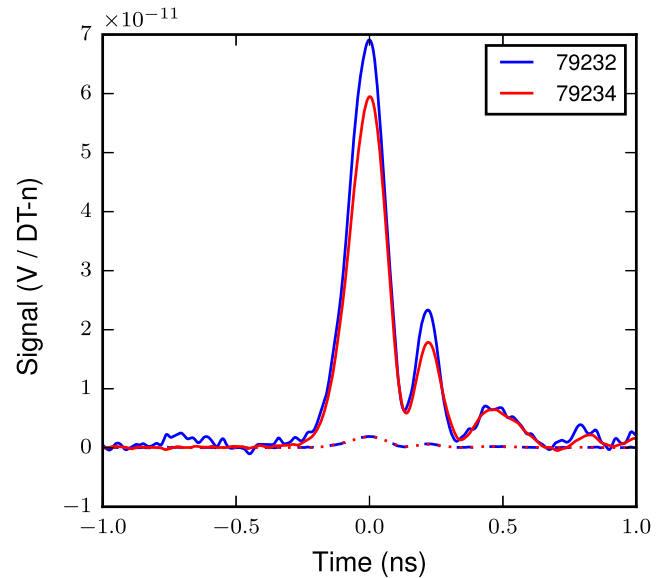


FIG. 4. Cherenkov signal from two  $\text{H}_2\text{T}_2$  fueled implosions: 79 232 (blue) and 79 234 (red). The signal is shown normalized to the DT neutron yield. The blue dashed and red dotted curves represent the signal contribution from DT- $\gamma$ 's alone, while the bulk of the signal is from HT- $\gamma$ 's. The GCD was run with 100 psi of  $\text{CO}_2$ .

absolute signal level is approximately consistent with the level expected from the radiation-hydrodynamic simulations. A detailed comparison of the yield, e.g., compared to the absolute DT yield, would require accounting for plasma effects including species separation,<sup>31–33</sup> which is beyond the scope of this work.

## IV. ANALYSIS OF MIXED HT AND DT SIGNALS

We consider two techniques to analyze the data with mixed HT and DT burn histories: first, using a reference shot with only one reaction, and second, performing a simultaneous forward fit to the differentially thresholded detectors.

### A. Relative shot-to-shot technique

An easy way to analyze mixed burn histories is by using a reference shot where only one is present. In this work, we have implosions with a nearly pure HT- $\gamma$  signal (see Fig. 4). By then conducting an otherwise identical implosion with D introduced into the target, generating dual burn, we can use the difference between the two shots to infer the signal contribution from DT- $\gamma$ 's.

Example data for this technique are shown in Fig. 5. First, an implosion with the pure HT- $\gamma$  signal, shot 80 345, is made forward fit using a Gaussian burn (source function). The forward fit does not exactly match the PMT ringing due to the uncertainties in the instrument response in that region.<sup>34</sup> The same HT source function is then used with an additional DT source function to forward fit the dual burn case (right, shot 80 348).

There are two major limitations to using this analysis: first, that it requires two shots per measurement, and second, that the precision of the temporal shift measurement between the HT and DT bang time depends upon the implosion

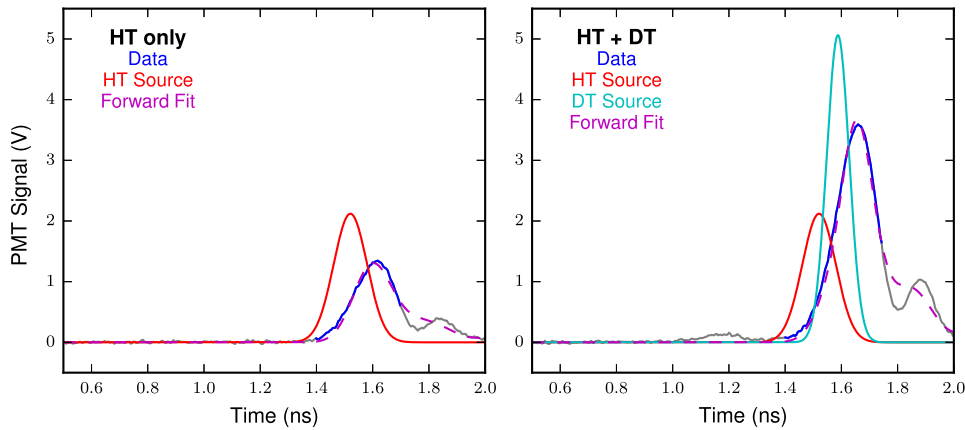


FIG. 5. Data from shot 80345 (left, HT- $\gamma$  only) and shot 80348 (right, both HT and DT). These data were taken with the GCD-1 detector with 100 psi (absolute) of  $\text{CO}_2$ . On the left, a HT source function is forward fitted to the data. A DT source function is then added to forward fit the mixed burn case (right). The data are plotted in gray with the region used for  $\chi^2$  minimization in blue.

repeatability and the HT reaction reproducibility. Empirically, nominally identical implosions of this type have measured bang times that vary by  $\pm 20$  ps ( $1\sigma$ ), which are taken as the major component of the uncertainty for this technique. An additional uncertainty is included from the  $\chi^2$  minimization during the forward fit.

For the data shown in Fig. 5, this method gives a difference between the DT and HT bang times (a peak of nuclear production) as  $\Delta T \equiv \text{BT}_{\text{HT}} - \text{BT}_{\text{DT}} = -67 \pm 21$  ps for shot 80348.

## B. Simultaneous forward fit

The limitations of the shot-to-shot analysis technique can be mitigated by performing a simultaneous forward fit to data from two differentially thresholded detectors on a single shot. The differentially thresholded detectors will have different sensitivities to the HT and DT  $\gamma$  rays (see Fig. 3). In this experiment, the GCD-1 detector was used with 100 psi (absolute) of  $\text{CO}_2$  gas, while the GCD-3 detector was used with 30 psi (absolute) of  $\text{CO}_2$ . In this configuration, GCD-3 is roughly as twice as sensitive to the HT- $\gamma$ 's. A fiducial signal from the laser system is used to co-register the oscilloscopes used for each instrument, providing relative timing corrections relative to a reference shot where the detectors were fielded at identical conditions.

The fitting analysis for shot 80348 is shown in Fig. 6. The Gaussian source functions for the nuclear burn of both HT and DT reactions are convolved with the instrument response to simultaneously fit the recorded GCD-1 and GCD-3 data. Since GCD-3 is more sensitive to the HT  $\gamma$  rays, a unique solution can be obtained. Because the instrument response is not well known after the main signal, due to the PMT ringing caused by a mismatched impedance, only the region around the peak is used in the fit  $\chi^2$  minimization (blue region). The complete data signals are shown in gray. The uncertainty in the relative bang time between the two nuclear reactions is calculated using the  $\chi^2$  fitting minimization routine. The source functions from this technique are similar to the source functions from the shot-to-shot technique (Fig. 5). For shot 80348, this analysis gives  $\Delta T \equiv \text{BT}_{\text{HT}} - \text{BT}_{\text{DT}} = -71 \pm 9$  ps.

## C. Comparison

A comparison of the difference in bang time ( $\Delta \text{BT}$ ) between the two reactions, as inferred using these techniques, is shown in Fig. 7. A set of four shots were conducted in which the HT fusion bang time was either early or late, compared to the DT bang time. As shown in Fig. 7, an excellent agreement between the two analysis techniques is found, demonstrating both self-consistency in the data set and the validity of the analysis.

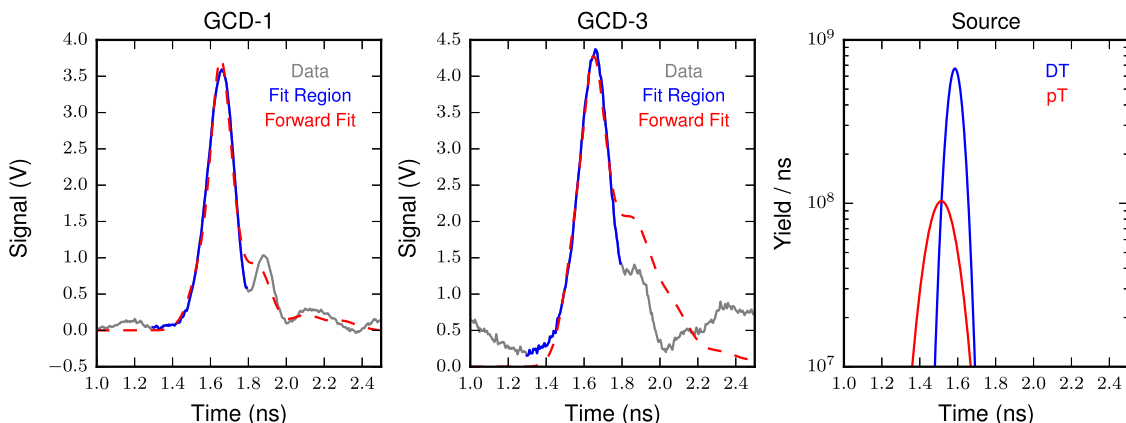


FIG. 6. Simultaneous forward fit analysis of shot 80348. The GCD-1 data [left, 100 psi (absolute)  $\text{CO}_2$ ] and GCD-3 data [center, 30 psi (absolute)  $\text{CO}_2$ ] are simultaneously fit using the source functions for DT and HT burn (right) convolved with the instrument response. The data are plotted in gray with the region used for  $\chi^2$  minimization in blue.

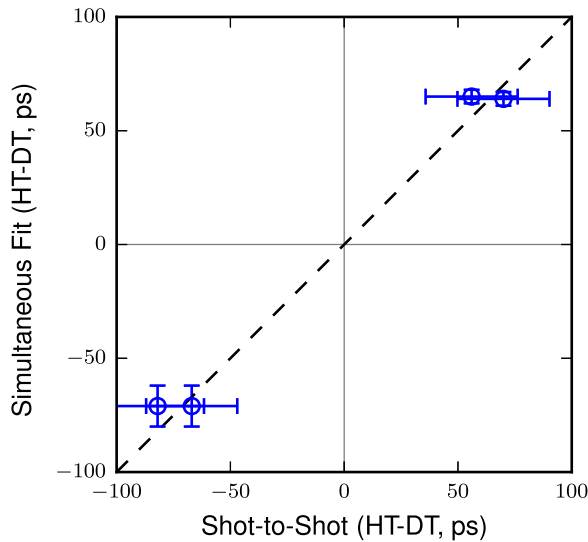


FIG. 7. Comparison of the differential bang time inferred using the two analysis techniques.

## V. CONCLUSIONS

Using Cherenkov detectors, the 19.8 MeV HT fusion  $\gamma$  ray has been observed in inertial fusion implosions for the first time. Because this  $\gamma$  ray is of higher energy than the DT fusion  $\gamma$ , it can be discriminated from the DT  $\gamma$  by using a higher threshold energy for the detector. This enables measurements of the fusion burn history of both reactions using differentially thresholded detectors. This technique has been demonstrated using implosions in the OMEGA laser facility, using shot-to-shot signal comparisons or a simultaneous forward fit to both detectors on a single shot. Good agreement is found between these analysis techniques, validating the measurement.

This technique requires comparable HT and DT  $\gamma$ -ray yields, within a factor of a few, which can be accomplished using deuterium-poor ( $\sim 2\%$ ) fuel mixtures. A higher dynamic range could be enabled using higher sensitivity detectors fielded at higher  $\gamma$ -ray thresholds, which would increase their relative sensitivity to the HT- $\gamma$ . The current data are also primarily sensitive to the difference in peak burn rate (bang time) between the reactions, limited by the PMT response ( $\sim 100$  ps); complete burn histories could be measured using faster PMTs.<sup>35</sup>

This technique enables important inertial fusion physics studies. First, mixing of the shell material into the hot spot can be a significant degradation mechanism. Several studies have used the separated reactant technique<sup>13,15–19</sup> to study the mix. This technique can be applied to  $H_2T_2$  fueled implosions with D doped into the ablator material to diagnose both the level and time evolution of the shell material mixing into the fuel. Another potential application is to the implosions that deviate from the hydrodynamic behavior, where multiple ion species fuels may segregate and cause discrepancies between nuclear bang times.<sup>31–33,36</sup>

## ACKNOWLEDGMENTS

We thank the operation crew and engineering staff at OMEGA for supporting these experiments, Tom Sedillo and

Robert Aragonez for support fielding the GCDs, and Jorge Sanchez at the LLNL Tritium Facility for supporting the target fuel filling. A.B.Z. gratefully acknowledges the support provided for this work by the Laboratory Directed Research and Development (LDRD) program, Project No. 20150717PRD2, at Los Alamos National Laboratory. This work was performed under the auspices of the U.S. Department of Energy by LANL under Contract No. DE-AC62-06NA25396.

<sup>1</sup>J. Nuckolls, L. Wood, A. Thiessen, and G. Zimmerman, *Nature* **239**, 139–142 (1972).

<sup>2</sup>O. A. Hurricane, D. A. Callahan, D. T. Casey, P. M. Celliers, C. Cerjan, E. L. Dewald, T. R. Dittrich, T. Doppner, D. E. Hinkel, L. F. B. Hopkins, J. L. Kline, S. Le Pape, T. Ma, A. G. MacPhee, J. L. Milovich, A. Pak, H. S. Park, P. K. Patel, B. A. Remington, J. D. Salmonson, P. T. Springer, and R. Tommasini, *Nature* **506**, 343–348 (2014).

<sup>3</sup>M. J. Edwards, P. K. Patel, J. D. Lindl, L. J. Atherton, S. H. Glenzer, S. W. Haan, J. D. Kilkenny, O. L. Landen, E. I. Moses, A. Nikroo, R. Petrasso, T. C. Sangster, P. T. Springer, S. Batha, R. Benedetti, L. Bernstein, R. Betti, D. L. Bleuel, T. R. Boehly, D. K. Bradley, J. A. Caggiano, D. A. Callahan, P. M. Celliers, C. J. Cerjan, K. C. Chen, D. S. Clark, G. W. Collins, E. L. Dewald, L. Divol, S. Dixit, T. Doeppner, D. H. Edgell, J. E. Fair, M. Farrell, R. J. Fortner, J. Frenje, M. G. Gatu Johnson, E. Giraldez, V. Y. Glebov, G. Grim, B. A. Hammel, A. V. Hamza, D. R. Harding, S. P. Hatchett, N. Hein, H. W. Herrmann, D. Hicks, D. E. Hinkel, M. Hoppe, W. W. Hsing, N. Izumi, B. Jacoby, O. S. Jones, D. Kalantar, R. Kauffmann, J. L. Kline, J. P. Knauer, J. A. Koch, B. J. Koziemiński, G. Kyrala, K. N. LaFortune, S. L. Pape, R. J. Leeper, R. Lerche, T. Ma, B. J. MacGowan, A. J. MacKinnon, A. MacPhee, E. R. Mapoles, M. M. Marinak, M. Mauldin, P. W. McKenty, M. Meezan, P. A. Michel, J. L. Milovich, J. D. Moody, M. Moran, D. H. Munro, C. L. Olson, K. Opachich, A. E. Pak, T. Parham, H.-S. Park, J. E. Ralph, S. P. Regan, B. Remington, H. Rinderknecht, H. F. Robey, M. Rosen, S. Ross, J. D. Salmonson, J. Sater, D. H. Schneider, F. H. Sguin, S. M. Sepke, D. A. Shaughnessy, V. A. Smalyuk, B. K. Spears, C. Stoeckl, W. Stoeffl, L. Suter, C. A. Thomas, R. Tommasini, R. P. Town, S. V. Weber, P. J. Wegner, K. Widman, M. Wilke, D. C. Wilson, C. B. Yeamans, and A. Zylstra, *Phys. Plasmas* **20**, 070501 (2013).

<sup>4</sup>O. A. Hurricane, D. A. Callahan, D. T. Casey, E. L. Dewald, T. R. Dittrich, T. Doppner, S. Haan, D. E. Hinkel, L. F. Berzak Hopkins, O. Jones, A. L. Kritcher, S. Le Pape, T. Ma, A. G. MacPhee, J. L. Milovich, J. Moody, A. Pak, H. S. Park, P. K. Patel, J. E. Ralph, H. F. Robey, J. S. Ross, J. D. Salmonson, B. K. Spears, P. T. Springer, R. Tommasini, F. Albert, L. R. Benedetti, R. Bionta, E. Bond, D. K. Bradley, J. Caggiano, P. M. Celliers, C. Cerjan, J. A. Church, R. Dylla-Spears, D. Edgell, M. J. Edwards, D. Fittinghoff, M. A. Barrios Garcia, A. Hamza, R. Hatari, H. Herrmann, M. Hohenberger, D. Hoover, J. L. Kline, G. Kyrala, B. Koziemiński, G. Grim, J. E. Field, J. Frenje, N. Izumi, M. Gatu Johnson, S. F. Khan, J. Knauer, T. Kohut, O. Landen, F. Merrill, P. Michel, A. Moore, S. R. Nagel, A. Nikroo, T. Parham, R. R. Rygg, D. Sayre, M. Schneider, D. Shaughnessy, D. Strozzi, R. P. J. Town, D. Turnbull, P. Volegov, A. Wan, K. Widmann, C. Wilde, and C. Yeamans, *Nat. Phys.* **12**, 800 (2016).

<sup>5</sup>G. H. Miller, E. Moses, and C. R. Wuest, *Nucl. Fusion* **44**, S228 (2004).

<sup>6</sup>E. Moses *et al.*, *Fusion Sci. Technol.* **69**, 1 (2016).

<sup>7</sup>T. Boehly, D. Brown, R. Craxton, R. Keck, J. Knauer, J. Kelly, T. Kessler, S. Kumpan, S. Loucks, S. Letzring *et al.*, *Opt. Commun.* **133**, 495–506 (1997).

<sup>8</sup>T. Ma, P. K. Patel, N. Izumi, P. T. Springer, M. H. Key, L. J. Atherton, L. R. Benedetti, D. K. Bradley, D. A. Callahan, P. M. Celliers, C. J. Cerjan, D. S. Clark, E. L. Dewald, S. N. Dixit, T. Doppner, D. H. Edgell, R. Epstein, S. Glenn, G. Grim, S. W. Haan, B. A. Hammel, D. Hicks, W. W. Hsing, O. S. Jones, S. F. Khan, J. D. Kilkenny, J. L. Kline, G. A. Kyrala, O. L. Landen, S. Le Pape, B. J. MacGowan, A. J. MacKinnon, A. G. MacPhee, N. B. Meezan, J. D. Moody, A. Pak, T. Parham, H.-S. Park, J. E. Ralph, S. P. Regan, B. A. Remington, H. F. Robey, J. S. Ross, B. K. Spears, V. Smalyuk, L. J. Suter, R. Tommasini, R. P. Town, S. V. Weber, J. D. Lindl, M. J. Edwards, S. H. Glenzer, and E. I. Moses, *Phys. Rev. Lett.* **111**, 085004 (2013).

<sup>9</sup>J. Lindl *et al.*, “Review of the National Ignition Campaign 2009–2012,” *Phys. Plasmas* **21**, 020501 (2014).

<sup>10</sup>G. Dimonte and R. Tipton, “K-L turbulence model for the self-similar growth of the Rayleigh-Taylor and Richtmyer-Meshkov instabilities,” *Phys. Fluids* **18**, 085101 (2006).

- <sup>11</sup>R. E. Chrien, N. M. Hoffman, J. D. Colvin, C. J. Keane, O. L. Landen, and B. A. Hammel, "Fusion neutrons from the gas-pusher interface in deuterated-shell inertial confinement fusion implosions," *Phys. Plasmas* **5**, 768–774 (1998).
- <sup>12</sup>C. K. Li, F. H. Séguin, J. A. Frenje, S. Kurebayashi, R. D. Petrasso, D. D. Meyerhofer, J. M. Soures, J. A. Delettrez, V. Y. Glebov, P. B. Radha, S. P. Regan, S. Roberts, T. C. Sangster, and C. Stoeckl, "Effects of fuel-shell mix upon direct-drive, spherical implosions on OMEGA," *Phys. Rev. Lett.* **89**, 165002 (2002).
- <sup>13</sup>J. R. Rygg, J. A. Frenje, C. K. Li, F. H. Séguin, R. D. Petrasso, V. Y. Glebov, D. D. Meyerhofer, T. C. Sangster, and C. Stoeckl, *Phys. Rev. Lett.* **98**, 215002 (2007).
- <sup>14</sup>D. C. Wilson, P. S. Ebey, T. C. Sangster, W. T. Shmayda, V. Y. Glebov, and R. A. Lerche, "Atomic mix in directly driven inertial confinement implosions," *Phys. Plasmas* **18**, 112707 (2011).
- <sup>15</sup>H. G. Rinderknecht, H. Sio, C. K. Li, A. B. Zylstra, M. J. Rosenberg, P. Amendt, J. Delettrez, C. Bellei, J. A. Frenje, M. Gatu Johnson, F. H. Séguin, R. D. Petrasso, R. Betti, V. Y. Glebov, D. D. Meyerhofer, T. C. Sangster, C. Stoeckl, O. Landen, V. A. Smalyuk, S. Wilks, A. Greenwood, and A. Nikroo, "First observations of nonhydrodynamic mix at the fuel-shell interface in shock-driven inertial confinement implosions," *Phys. Rev. Lett.* **112**, 135001 (2014).
- <sup>16</sup>V. A. Smalyuk, R. E. Tipton, J. E. Pino, D. T. Casey, G. P. Grim, B. A. Remington, D. P. Rowley, S. V. Weber, M. Barrios, L. R. Benedetti, D. L. Bleuel, D. K. Bradley, J. A. Caggiano, D. A. Callahan, C. J. Cerjan, D. S. Clark, D. H. Edgell, M. J. Edwards, J. A. Frenje, M. Gatu-Johnson, V. Y. Glebov, S. Glenn, S. W. Haan, A. Hamza, R. Hatarik, W. W. Hsing, N. Izumi, S. Khan, J. D. Kilkenny, J. Kline, J. Knauer, O. L. Landen, T. Ma, J. M. McNaney, M. Mintz, A. Moore, A. Nikroo, A. Pak, T. Parham, R. Petrasso, D. B. Sayre, M. B. Schneider, R. Tommasini, R. P. Town, K. Widmann, D. C. Wilson, and C. B. Yeaman, *Phys. Rev. Lett.* **112**, 025002 (2014).
- <sup>17</sup>V. A. Smalyuk, M. Barrios, J. A. Caggiano, D. T. Casey, C. J. Cerjan, D. S. Clark, M. J. Edwards, J. A. Frenje, M. Gatu-Johnson, V. Y. Glebov, G. Grim, S. W. Haan, B. A. Hammel, A. Hamza, D. E. Hoover, W. W. Hsing, O. Hurricane, J. D. Kilkenny, J. L. Kline, J. P. Knauer, J. Kroll, O. L. Landen, J. D. Lindl, T. Ma, J. M. McNaney, M. Mintz, A. Moore, A. Nikroo, T. Parham, J. L. Peterson, R. Petrasso, L. Pickworth, J. E. Pino, K. Raman, S. P. Regan, B. A. Remington, H. F. Robey, D. P. Rowley, D. B. Sayre, R. E. Tipton, S. V. Weber, K. Widmann, D. C. Wilson, and C. B. Yeaman, *Phys. Plasmas* **21**, 056301 (2014).
- <sup>18</sup>S. V. Weber, D. T. Casey, D. C. Eder, J. D. Kilkenny, J. E. Pino, V. A. Smalyuk, G. P. Grim, B. A. Remington, D. P. Rowley, C. B. Yeaman, R. E. Tipton, M. Barrios, R. Benedetti, L. Berzak Hopkins, D. L. Bleuel, E. J. Bond, D. K. Bradley, J. A. Caggiano, D. A. Callahan, C. J. Cerjan, D. S. Clark, L. Divol, D. H. Edgell, M. J. Edwards, M. J. Eckart, D. Fittinghoff, J. A. Frenje, M. Gatu-Johnson, V. Y. Glebov, S. Glenn, N. Guler, S. W. Haan, A. Hamza, R. Hatarik, H. Herrmann, D. Hoover, W. W. Hsing, N. Izumi, O. S. Jones, M. Kervin, S. Khan, J. Kline, J. Knauer, A. Kritcher, G. Kyrala, O. L. Landen, S. L. Pape, T. Ma, A. J. Mackinnon, A. G. MacPhee, M. M. Marinak, J. M. McNaney, N. B. Meezan, F. E. Merrill, M. Mintz, A. Moore, D. H. Munro, A. Nikroo, A. Pak, T. Parham, R. Petrasso, H. G. Rinderknecht, D. B. Sayre, S. M. Sepke, B. K. Spears, W. Stoeffl, R. Tommasini, R. P. Town, P. Volegov, K. Widmann, D. C. Wilson, and A. B. Zylstra, *Phys. Plasmas* **21**, 112706 (2014).
- <sup>19</sup>D. T. Casey, V. A. Smalyuk, R. E. Tipton, J. E. Pino, G. P. Grim, B. A. Remington, D. P. Rowley, S. V. Weber, M. Barrios, L. R. Benedetti, D. L. Bleuel, E. J. Bond, D. K. Bradley, J. A. Caggiano, D. A. Callahan, C. J. Cerjan, K. C. Chen, D. H. Edgell, M. J. Edwards, D. Fittinghoff, J. A. Frenje, M. Gatu-Johnson, V. Y. Glebov, S. Glenn, N. Guler, S. W. Haan, A. Hamza, R. Hatarik, H. W. Herrmann, D. Hoover, W. W. Hsing, N. Izumi, P. Kervin, S. Khan, J. D. Kilkenny, J. Kline, J. Knauer, G. Kyrala, O. L. Landen, T. Ma, A. G. MacPhee, J. M. McNaney, M. Mintz, A. Moore, A. Nikroo, A. Pak, T. Parham, R. Petrasso, H. G. Rinderknecht, D. B. Sayre, M. Schneider, W. Stoeffl, R. Tommasini, R. P. Town, K. Widmann, D. C. Wilson, and C. B. Yeaman, *Phys. Plasmas* **21**, 092705 (2014).
- <sup>20</sup>Y. Kim, J. M. Mack, H. W. Herrmann, C. S. Young, G. M. Hale, S. Caldwell, N. M. Hoffman, S. C. Evans, T. J. Sedillo, A. McEvoy, J. Langenbrunner, H. H. Hsu, M. A. Huff, S. Batha, C. J. Horsfield, M. S. Rubery, W. J. Garbett, W. Stoeffl, E. Grafil, L. Bernstein, J. A. Church, D. B. Sayre, M. J. Rosenberg, C. Waugh, H. G. Rinderknecht, M. Gatu Johnson, A. B. Zylstra, J. A. Frenje, D. T. Casey, R. D. Petrasso, E. Kirk Miller, V. Yu Glebov, C. Stoeckl, and T. C. Sangster, *Phys. Plasmas* **19**, 056313 (2012).
- <sup>21</sup>C. E. Parker, C. R. Brune, T. N. Massey, J. E. O'Donnell, A. L. Richard, and D. B. Sayre, "The  ${}^3\text{H}(d,\gamma){}^5\text{He}$  reaction for  $E_{c.m.} \leq 300$  keV," *EPJ Web Conf.* **113**, 03005 (2016).
- <sup>22</sup>F. E. Cecil, D. M. Cole, R. Philbin, N. Jarmie, and R. E. Brown, "Reaction  ${}^2\text{H}({}^3\text{He},\gamma){}^5\text{Li}$  at center-of-mass energies between 25 and 60 keV," *Phys. Rev. C* **32**, 690–693 (1985).
- <sup>23</sup>F. J. Wilkinson and F. E. Cecil, " ${}^2\text{H}(d,\gamma){}^4\text{He}$  reaction at low energies," *Phys. Rev. C* **31**, 2036–2040 (1985).
- <sup>24</sup>K. I. Hahn, C. R. Brune, and R. W. Kavanagh, " ${}^3\text{H}(p,\gamma){}^4\text{He}$  cross section," *Phys. Rev. C* **51**, 1624–1632 (1995).
- <sup>25</sup>D. Tilley, H. Weller, and G. Hale, "Energy levels of light nuclei  $A = 4$ ," *Nucl. Phys. A* **541**, 1–104 (1992).
- <sup>26</sup>J. Mack, R. Berggren, S. Caldwell, S. Evans, J. Faulkner, Jr., R. Lerche, J. Oertel, and C. Young, *Nucl. Instrum. Methods Phys. Res., Sect. A* **513**, 566–572 (2003).
- <sup>27</sup>H. W. Herrmann, C. S. Young, J. M. Mack, Y. H. Kim, A. McEvoy, S. Evans, T. Sedillo, S. Batha, M. Schmitt, D. C. Wilson, J. R. Langenbrunner, R. Malone, M. I. Kaufman, B. C. Cox, B. Frogget, E. K. Miller, Z. A. Ali, T. W. Tunnell, W. Stoeffl, C. J. Horsfield, and M. Rubery, *J. Phys.: Conf. Ser.* **244**, 032047 (2010).
- <sup>28</sup>M. S. Rubery, C. J. Horsfield, H. Herrmann, Y. Kim, J. M. Mack, C. Young, S. Evans, T. Sedillo, A. McEvoy, S. E. Caldwell, E. Grafil, W. Stoeffl, and J. S. Milnes, *Rev. Sci. Instrum.* **84**, 073504 (2013).
- <sup>29</sup>H. W. Herrmann, Y. H. Kim, C. S. Young, V. E. Fatherley, F. E. Lopez, J. A. Oertel, R. M. Malone, M. S. Rubery, C. J. Horsfield, W. Stoeffl, A. B. Zylstra, W. T. Shmayda, and S. H. Batha, *Rev. Sci. Instrum.* **85**, 11E124 (2014).
- <sup>30</sup>C. J. Forrest, P. B. Radha, V. Y. Glebov, V. N. Goncharov, J. P. Knauer, A. Pruyne, M. Romanofsky, T. C. Sangster, M. J. Shoup, C. Stoeckl, D. T. Casey, M. Gatu-Johnson, and S. Gardner, *Rev. Sci. Instrum.* **83**, 10D919 (2012).
- <sup>31</sup>J. R. Rygg, J. A. Frenje, C. K. Li, F. H. Sguin, R. D. Petrasso, J. A. Delettrez, V. Y. Glebov, V. N. Goncharov, D. D. Meyerhofer, S. P. Regan, T. C. Sangster, and C. Stoeckl, *Phys. Plasmas* **13**, 052702 (2006).
- <sup>32</sup>H. W. Herrmann, J. R. Langenbrunner, J. M. Mack, J. H. Cooley, D. C. Wilson, S. C. Evans, T. J. Sedillo, G. A. Kyrala, S. E. Caldwell, C. S. Young, A. Nobile, J. Wermer, S. Paglieri, A. M. McEvoy, Y. Kim, S. H. Batha, C. J. Horsfield, D. Drew, W. Garbett, M. Rubery, V. Y. Glebov, S. Roberts, and J. A. Frenje, *Phys. Plasmas* **16**, 056312 (2009).
- <sup>33</sup>D. T. Casey, J. A. Frenje, M. Gatu Johnson, M. J.-E. Manuel, H. G. Rinderknecht, N. Sinenian, F. H. Séguin, C. K. Li, R. D. Petrasso, P. B. Radha, J. A. Delettrez, V. Y. Glebov, D. D. Meyerhofer, T. C. Sangster, D. P. McNabb, P. A. Amendt, R. N. Boyd, J. R. Rygg, H. W. Herrmann, Y. H. Kim, and A. D. Bacher, *Phys. Rev. Lett.* **108**, 075002 (2012).
- <sup>34</sup>The instrument response, particularly the ringing behavior, depends upon the light illumination pattern on the PMT, which is known to be different between the response characterization system and the Cherenkov instrument.
- <sup>35</sup>J. D. Hares, A. K. L. Dymoke-Bradshaw, T. J. Hilsabeck, J. D. Kilkenny, D. Morris, C. J. Horsfield, S. G. Gales, J. Milnes, H. W. Herrmann, and C. McFee, *J. Phys.: Conf. Ser.* **717**, 012093 (2016).
- <sup>36</sup>H. G. Rinderknecht, M. J. Rosenberg, C. K. Li, N. M. Hoffman, G. Kagan, A. B. Zylstra, H. Sio, J. A. Frenje, M. Gatu Johnson, F. H. Séguin, R. D. Petrasso, P. Amendt, C. Bellei, S. Wilks, J. Delettrez, V. Y. Glebov, C. Stoeckl, T. C. Sangster, D. D. Meyerhofer, and A. Nikroo, *Phys. Rev. Lett.* **114**, 025001 (2015).